Characterization of Polymer-Layered Silicate (Clay) Nanocomposites by Transmission Electron Microscopy and X-Ray Diffraction: A Comparative Study

Alexander B. Morgan, Jeffrey W. Gilman

Fire Science Division, Building and Fire Research Laboratory, National Institute of Standards and Technology, Gaithersburg, Maryland 20899

Received 4 December 2001; accepted 21 February 2002

ABSTRACT: Several polymer-layered silicate (clay) nanocomposites (PLSNs) were analyzed by transmission electron microscopy (TEM) and wide-angle X-ray diffraction (XRD) in an effort to characterize the nanoscale dispersion of the layered silicate. The PLSNs investigated included thermoset (cyanate esters) and thermoplastic polymers (polystyrene, nylon 6, and polypropylene-*g*-maleic anhydride). The results of this study reveal that the overall nanoscale dispersion of the clay in the polymer is best described by TEM, especially when mixed morphologies are present. XRD is useful for the measurement of *d*-spacings in intercalated systems but cannot always observe low clay loadings (<5%) or be used as a method to identify an exfoliated nanocomposite where no XRD peaks are present (constituting a negative result). Most importantly, the study showed that XRD is not a stand-alone technique, and it should be used in conjunction with TEM. Our studies suggest that new definitions, or a clarification of existing definitions, are needed to properly describe the diversity of PLSN nanostructures seen in various materials. © 2002 Wiley Periodicals, Inc.* J Appl Polym Sci 87: 1329–1338, 2003

Key words: nanocomposites; WAXS; TEM

INTRODUCTION

The study of polymer-layered silicate nanocomposites (PLSNs) is currently an expanding field of research because PLSNs often exhibit a wide range of improved properties over their unmodified starting polymers. The improved properties for these nanocomposites include mechanical,[1–4] thermal,[1–4] and flammability properties[4–7] and are related to the dispersion and nanostructure of the layered silicate in the polymer. The greatest improvement of benefits comes with exfoliated samples,[1–4] with the exception of flammability properties, where both exfoliated and intercalated materials seem to behave in the same manner.[5,6] There are several techniques that are used to elucidate the nanostructure of PLSNs, including atomic force microscopy,[8] NMR,[9–11] and neutron-scattering methods;[12] however, wide-angle X-ray diffraction (XRD)[1–4,13] and transmission electron microscopy (TEM)[1–4,14–16] are the most commonly used techniques.

There is a wide range of layered silicates available, but only a few have found use in PLSN materials. Before one can give a detailed explanation of the PLSN structure, one must describe the chemistry of the layered silicate material. The most commonly used layered silicate in PLSNs is montmorillonite (MMT), an aluminosilicate smectite clay. This clay mineral is used because it is a cation-poor layered silicate, with layers that can be easily separated, or delaminated. More exactly, this clay has a low cation-exchange capacity and, therefore, does not have a large amount of ionic interactions holding the clay plates together. Cation-rich clay species, such as vermiculite, are difficult to delaminate, and the ease of delamination becomes important in modification of the clay.[17] These clays have a large amount of anionic sites in each plate charge balanced with group I or group II metal cations. Organic modification of MMT occurs by ion exchange of the sodium ions present on natural MMT with organic alkyl ammonium ions. This makes the normally hydrophilic clay hydrophobic and potentially more compatible with the polymer being used in

Correspondence to: A. B. Morgan, Inorganic Materials Group, Corporate R&D, The Dow Chemical Company, Midland, MI 48674 (abmorgan@dow.com).

Certain commercial equipment, instruments, materials, and companies are identified in this article to adequately specify the experimental procedure. This in no way implies endorsement or recommendation by the National Institute of Standards and Technology.

Contract grant sponsor: Federal Aviation Administration; contract grant number: DTFA 03-99-X-9009.

Contract grant sponsor: Flammability of Polymer–Clay Nanocomposites Consortium.

Journal of Applied Polymer Science, Vol. 87, 1329–1338 (2003)

preparation of the PLSN.[1,12] After the clay is organically modified, the most common technique used to analyze the clay is XRD, which allows the interlayer *d*-spacing (the distance between the basal layers of the MMT clay, or of any layered material) to be measured. Increased spacing between basal layers and a hydrophobic, organophilic surface make it more likely for the polymer to enter between the layers (referred to as the *gallery*) of the clay.[12,18] Because XRD has been successfully used to analyze organically modified clays, it has been employed to look at changes in *d*-spacings when PLSN materials are prepared. The *d*-spacing observed by XRD for PLSN materials has been used to describe the nanoscale dispersion of the clay in the polymer.[1] This has led to three definitions of the clay structures used to describe the dispersion of the clay in the PLSN. The three definitions used are immiscible, intercalated, and exfoliated (also referred to as *delaminated*). With XRD, *immiscible* materials have no change in *d*-spacing, meaning that no polymer has entered the gallery and that the spacing between clay layers is unchanged. *Intercalated* nanocomposites have an increased *d*-spacing, indicating that polymer has entered the gallery, expanding the layers. *Exfoliated* PLSNs show no peak by XRD, suggesting that a great amount of polymer has entered the gallery space, expanding the clay layers so far apart that diffraction cannot be observed with wide-angle ($2\theta > 1°$) XRD techniques. Furthermore, the clay layers are sufficiently disordered such that they no longer give a coherent XRD signal.[†]

There are many factors that influence the nanostructure of PLSNs. The organic treatment of the clay is one of the most important, as the organic treatment is essential for dispersing the normally hydrophilic clay into a hydrophobic polymer.[1,12] The thermal stability of the organic treatment is of importance, as many PLSNs (including some presented herein) are melt-blended or cured at high temperatures to yield a PLSN. This becomes important as the alkyl ammonium ion commonly used as the organic treatment for layered silicates is thermally unstable, typically decomposing at temperatures of 200°C or less.[7,19–21] When this decomposition occurs, the silicate layers become hydrophilic again, and their ability to positively affect physical properties may be reduced. The benefits (on mechanical, thermal, or flammability properties) usually gained from the PLSN are typically degraded under these conditions. Other factors, such as processing[22] and synthetic method[1,23–25] also have an effect on the nanostructure of the layered silicate in the PLSN.

[†]Wide-angle XRD is usually considered to be at angles (2θ) of 1° or higher. Angles below 1° are measured with small-angle XRD.

Recent work in our laboratory used both TEM and XRD to characterize the nanoscale dispersion of clay in a variety of PLSN materials. We found TEM to be an excellent qualitative method in the characterization of PLSNs, many of which may have a mixed morphology (regions of both exfoliated and intercalated nanostructures). XRD is most useful for the measurement of the *d*-spacing of ordered immiscible and ordered intercalated PLSNs, but it may be insufficient for the measurement of disordered and exfoliated materials that give no peak. More specifically, the lack of peak may be misinterpreted in cases where no peak is seen. Many factors, such as concentration and order of the clay, can influence the XRD patterns of layered silicates. For example, samples where the clay is not well ordered will fail to produce a Bragg diffraction peak, and that is the correct conclusion of the data. It is not the fault of the technique that leads to the incorrect conclusion of a nanocomposite being exfoliated when in reality it is highly disordered. Therefore, the lack of a peak obtained during XRD analysis merely states that no peak was observed; it does not prove, or disprove, the existence of exfoliated clay plates in the nanocomposite. We previously gave a preliminary report of the inability of XRD to properly identify differences between exfoliated and immiscible samples for cyanate esters.[26] This suggests that some samples listed in the literature, from studies that have only used XRD to analyze the nanocomposite materials, may be disordered (immiscible or intercalated) rather than exfoliated.[27,28] XRD results can be misinterpreted for intercalated and immiscible PLSNs that show peaks by XRD due to sampling problems, orientation, and poor calibration of most XRD instruments at very low angles.[29] TEM analysis on polyetherimide nanocomposites revealed that the material that was originally identified as immiscible by XRD had a large number of exfoliated single layers present, and the material that was shown to be intercalated had both exfoliated single layers and intercalated regions present.[30] The reason for these unusual structures was a result of the solution polymerization used to prepare these materials. In the previously mentioned study, and as this article also suggests, TEM and XRD become complimentary techniques, filling in gaps of information that other technique cannot obtain.

In this article, we address the characterization issues that occur when PLSNs are analyzed with XRD and TEM analysis. Both thermoplastic [polypropylene, polyamide-6, polystyrene (PS)] and thermoset (cyanate esters) PLSNs are discussed. A comparison of the data collected on each material with XRD and TEM is addressed. Finally, we address the differences between XRD and TEM analysis for PLSNs and inform the reader of the need for care when XRD data alone is used. These definitions for PLSNs are based on XRD results, which only describe the relationship

between clay layers in the polymer, not the relationship of the clay to the polymer. Therefore, TEM becomes a very powerful tool for the analysis of PLSNs, as it can describe qualitatively how the layered silicate is dispersed in the polymer. The TEM images in this article illustrate new, more comprehensive definitions for PLSNs, giving a general example of what each type of PLSN will look like when analyzed by TEM. Most importantly, the article shows how XRD and TEM can be used together to properly characterize PLSN materials.

EXPERIMENTAL

The synthesis of specific PLSNs (cyanate esters),[31] PS,[32] polypropylene-*g*-maleic anhydride (PPgMA),[15] and nylon 6 (PA-6)[33] in this study are described elsewhere.

XRD

XRD data were collected on a Philips diffractometer with Cu Kα radiation (λ = 0.1505945 nm) with a 0.02 2θ step size and a 2-s count time with a 0.066° slit width.[‡] Samples used for XRD were ground to a particle size of less than 40 μm with the exception of the PPgMA sample. The PPgMA materials were compression molded to give a solid monolith (14 mm × 14 mm × 2 mm thick) and were placed in a vertical configuration (transmission) for the collection of XRD data.

TEM

All samples were ultramicrotomed with a diamond knife on a Leica Ultracut UCT microtome (Bannockburn, IL) at either room temperature (cyanate esters and PS) or at −110°C (PPgMA and PA-6) to give sections with a nominal thickness of 70 nm. The sections were transferred from water (room temperature) or dry conditions (−110°C) to carbon-coated 200-mesh Cu grids. Bright-field TEM images of PLSNs (except for PA-6) were obtained at 120 kV, under low-dose conditions, with a Philips 400T electron microscope and with Kodak SO-161 film. Low-magnification images were taken at 2,800 and 10,000×. High-magnification images were taken at 28,000 and 60,000×. Bright-field TEM images of PA-6 nanocomposites were obtained at 120 kV, under low-dose conditions, with a Philips CM-12 electron microscope, and were digitally imaged with a charge coupled device (CCD) camera. High-magnification images (60,000×) could not be obtained with the CCD as the resolution of CCD digital cameras at this magnification is rather limited. We sampled the materials by taking several images of various magnifications over two to three sections per grid to ensure that analysis was based on a representative region of the sample.

[‡]This particular slit width helps prevent distortion of low-angle peaks (1° 2 θ to 15° 2θ) that can occur with finite-slit-width XRD experiments. However, with the use of smaller slit widths, longer count times must be used to make up for the loss in signal that is caused by the small slit width.

RESULTS AND DISCUSSION

Immiscible PLSNs

One of the nanocomposites we investigated was a novalac-based cyanate ester nanocomposite. XRD data obtained on the cyanate ester nanocomposites (with a solid monolith sample) showed no peak, suggesting exfoliation (Fig. 1). However, TEM analysis showed that the material was immiscible. Very large, unevenly dispersed primary clay particles (tactoids) were observed in the polymer at low magnification (Fig. 2), strongly suggesting an immiscible dispersion. Due to the poor dispersion of the primary clay particles, it is possible that the cyanate ester sample was not a nanocomposite but rather a traditional filled composite, with the clay particles, whose scale was in micrometers rather than nanometers, serving as the filler. The sample may be better defined as a microcomposite rather than as an immiscible nanocomposite. The PLSN that gave a peak by XRD used an MMT treated with quaternary alkyl ammonium (dimethyl dihydrogenated tallow ammonium; A–MMT) at a mass fraction of 10% loading. High magnification of this material (Fig. 3) showed that it had maintained order, whereas the polymer intercalated in between the MMT layers (referred to as the gallery space). The PLSN that showed no peak corresponding to *d*-spacings between 1° 2θ and 10° 2θ by XRD contained a mass fraction of 10% MMT clay, where the organic treatment was a melamine ammonium salt (MEL–MMT). Although the MMT stacks observed at high magnification by TEM (Fig. 4) did not appear as neatly ordered as the A–MMT nanocomposite, they were ordered enough that they should have given some sort of *d*-spacing. After observing this result, the cyanate esters were ground to a powder and analyzed by XRD again. This time, peaks were seen for the MEL–MMT sample, but they were quite faint [Fig. 1(b)]. Because the *d*-spacing was unchanged for this sample, it was considered immiscible. On the basis of this result, the nature of the sample (powder or solid) became a factor when XRD analysis was used. This type of phenomena is well known in XRD analysis, in that there may be a preferred orientation of crystallites in solid samples and that this orientation may be removed when the sample is converted to a powder. Because clay plates are known to align on injection molding,[21] this becomes a very important issue for the performance of XRD analysis on injection-molded parts. Therefore,

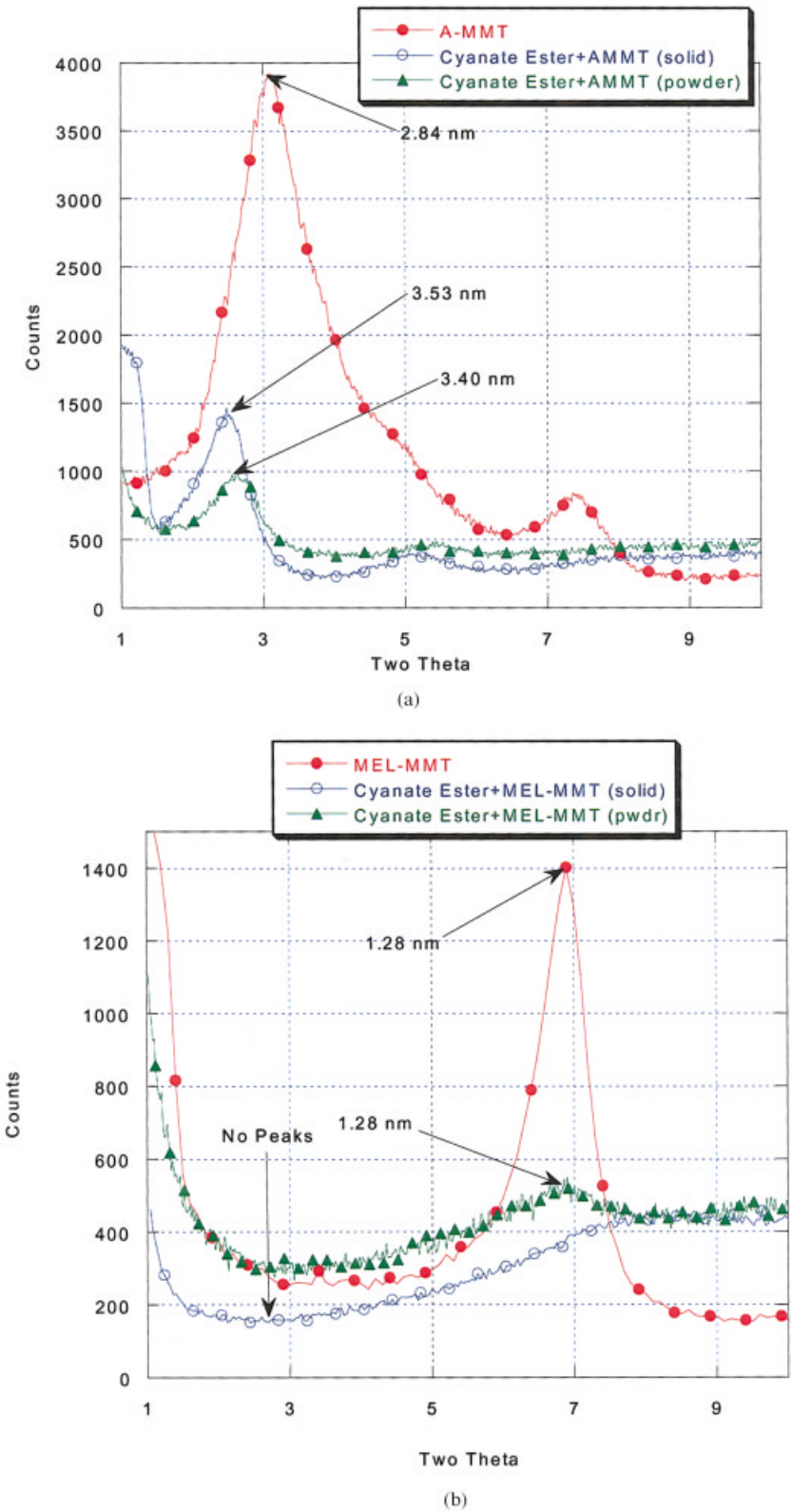

Figure 1 XTD plot of novalac-based cyanate ester nanocomposites (powder and solid samples). All samples contained a mass fraction of 10% layered silicate: (a) A–MMT and (b) MEL–MMT.

researchers are cautioned to consider these issues when performing XRD analysis on solid monolith PLSNs. Because some thermoplastics cannot be easily powdered due to high impact strengths or glass-transitions below room temperature, cryogrinding is recommended. However, in the case of the previous cy-

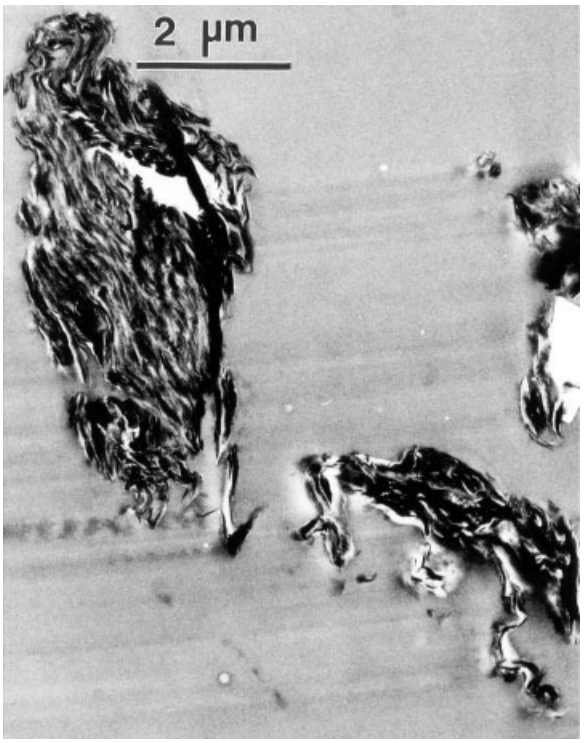

Figure 2 Low-magnification TEM image of an immiscible novalac-based cyanate ester nanocomposite (mass fraction = 10% MEL–MMT) that gave no peak by XRD.

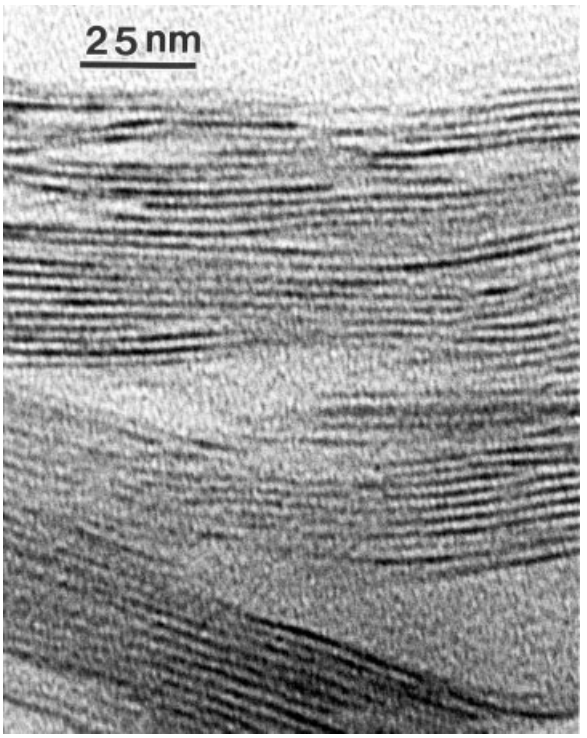

Figure 3 High-magnification TEM image of a novalac-based cyanate ester nanocomposite (mass fraction = 10% A–MMT) that gave a peak by XRD.

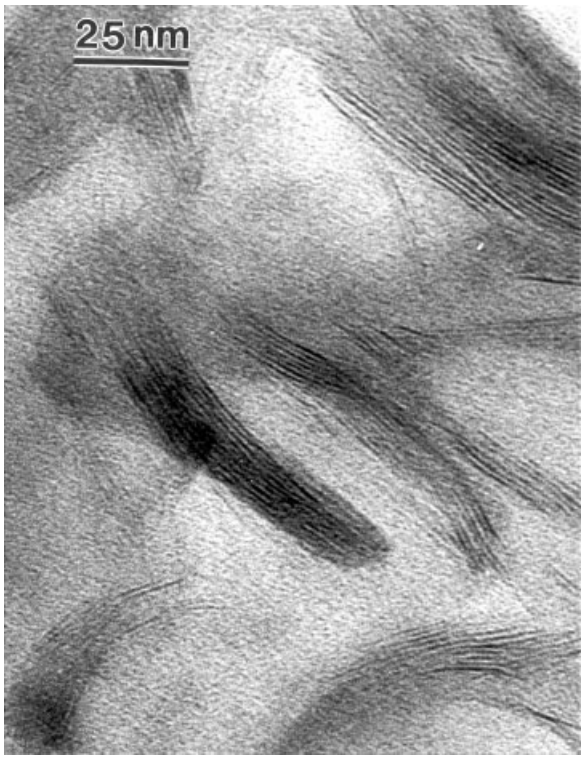

Figure 4 High-magnification TEM image of a novalac-based cyanate ester nanocomposite (mass fraction = 10% MEL–MMT) that gave no peak by solid-sample XRD but did when the sample was powdered.

anate ester MEL–MMT sample, which was not injection molded, the sampling issue that occurred was unexpected.

Intercalated/exfoliated PLSNs

The majority of PLSNs that we investigated were best described as intercalated/exfoliated. By XRD, they would be simply defined as intercalated, in that there was an observed increase in the *d*-spacing as compared to the original clay *d*-spacing. However, the TEM images showed that although there were indeed intercalated multilayer crystallites present, single exfoliated silicate layers were also prevalent, hence, the designation of an intercalated/exfoliated type of PLSNs. The two PLSNs discussed here are PS and PPgMA nanocomposites. Both of these materials were prepared via melt processing, either in a twin-screw extruder (PS) or in a mixing head (PPgMA). XRD showed the increased *d*-spacing for the intercalated fraction of clay present in these materials (Fig. 5), but the TEM images revealed a mixed morphology of intercalated and exfoliated structures. The broadness of the peak suggests that a diversity of structures existed, but this could have also been an effect of the local clay disorder within those crystallites. As pure exfoliated structures would not give peaks by XRD

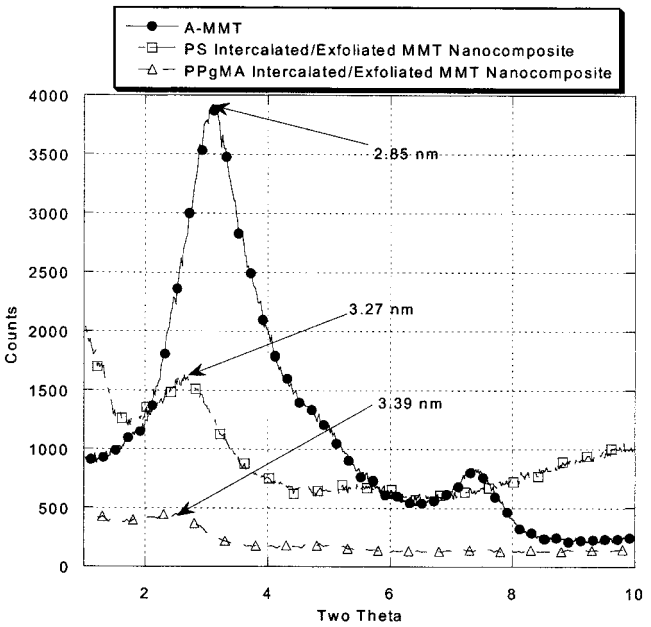

Figure 5 XRD plot of PS (mass fraction = 5% A–MMT) and PPgMA (mass fraction = 8% A–MMT) nanocomposite samples.

and when one keeps in mind that the absence of a peak is merely an absence of a peak and not proof of exfoliation, these results benefitted from the use of both XRD and TEM techniques. For the PS samples,

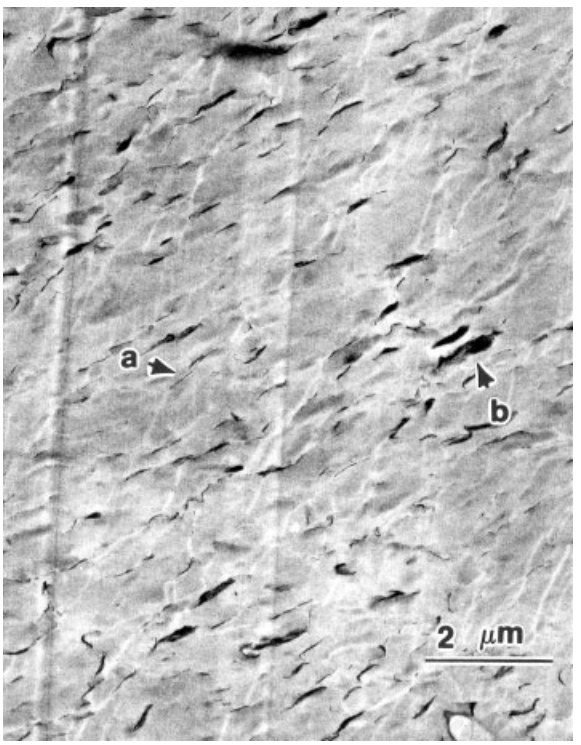

Figure 6 Low-magnification TEM image of an intercalated/exfoliated PS nanocomposite (mass fraction = 5% A–MMT). Both (a) small and (b) large tactoids were present.

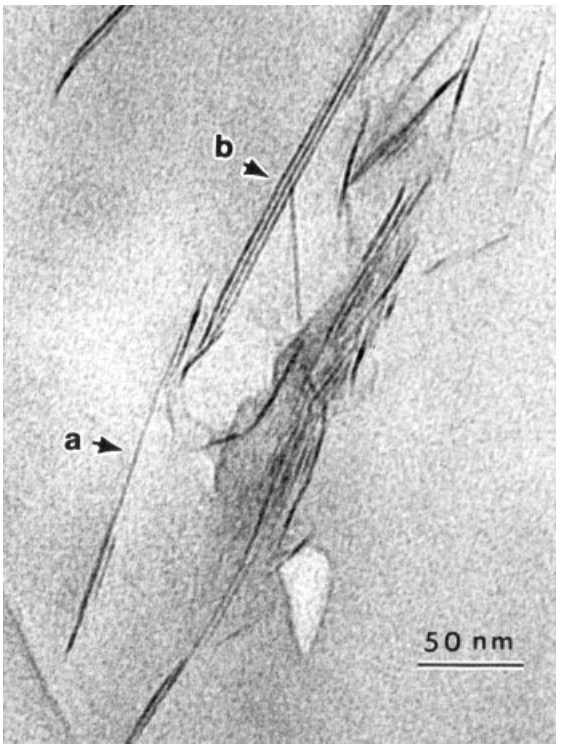

Figure 7 High-magnification TEM image of an intercalated/exfoliated PS nanocomposite (mass fraction = 5% A–MMT). (a) Exfoliated single layers and (b) small intercalated clay layer tactoids were present.

the low-magnification TEM image (Fig. 6) showed the clay to be well dispersed throughout the polymer. Higher magnification showed regions where both intercalated and exfoliated structures existed (Fig. 7) and regions where both intercalated tactoids and a few individual layers were present (Fig. 8). For the PPgMA samples, low magnification also showed that the clay was well dispersed (Fig. 9), and high magnification showed a region typical for this sample, with exfoliated clay layers and intercalated tactoids present (Fig. 10). Between the low-magnification images for the PS and PPgMA samples, there was a differing amount of orientation for each material. The PS sample, which had a mass fraction of 5% A–MMT, appeared to be more oriented and showed a sharper, but still broad, peak by XRD (Fig. 5). The PPgMA sample was much less oriented, and the XRD peak observed was very broad and low in intensity, despite a higher clay loading (mass fraction = 8% A–MMT). There appeared to be a larger number of exfoliated single MMT layers present in the PPgMA sample; thus, the proportion of remaining intercalated MMT stacks was still quite low. This may explain why the peak observed by XRD for this material, even at a MMT mass fraction of 8%, was smaller in height. Sample preparation in regards to XRD of these samples should also be considered. Shear used in sample preparation has been shown to induce order in PLSNs.[21] The PS sam-

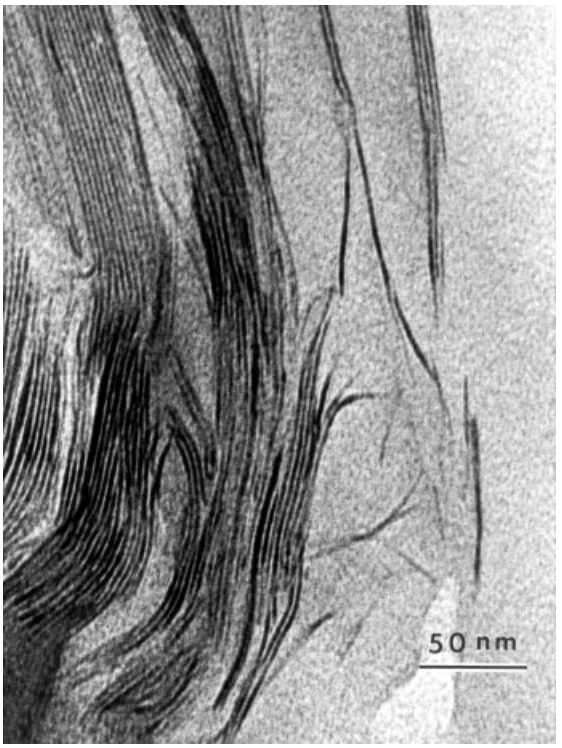

Figure 8 High-magnification TEM image of an intercalated/exfoliated PS nanocomposite (mass fraction = 5% A–MMT). This is a different region of the same sample shown in Figure 6, illustrating a large intercalated region.

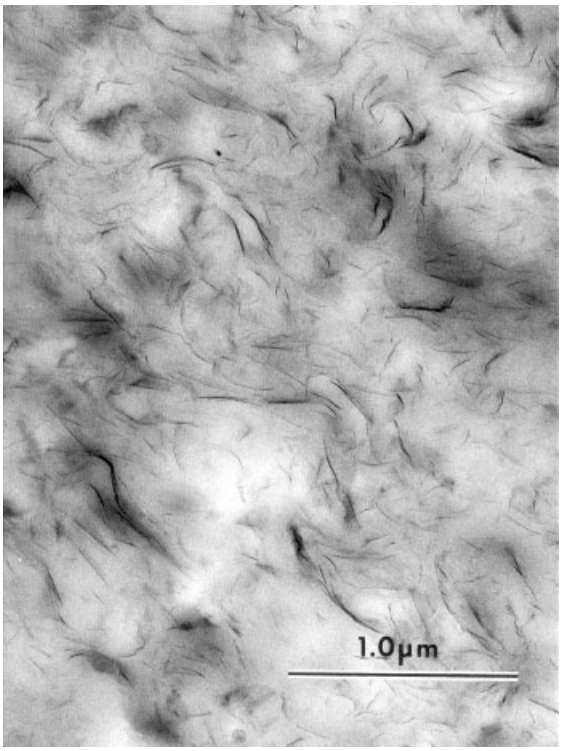

Figure 9 Low-magnification TEM image of a PPgMA intercalated/exfoliated nanocomposite (mass fraction = 8% A–MMT).

ple was easily ground into a powder, whereas the PPgMA could not be ground and was analyzed as a solid monolith. Given the result observed with the previous cyanate esters when the solid monolith samples were compared to powders used in XRD, the low intensity broad peak seen with the PPgMA sample may have also been an effect of the sample preparation. Peak broadening can also be caused by the clay itself, due to defects and lattice strain in the clay itself,[34] as well as finite distribution of clay stack sizes.[35]

Exfoliated PLSNs

We observed fully exfoliated morphologies in PLSNs, comprised of PS and PA-6. However, the two samples discussed here (PA-6 and PS) had much different nanostructures. TEM analyses of PS and PA-6 showed that single clay layers were in abundance throughout the polymer (Figs. 11 and 12, respectively) and spaced such that an XRD signal would not be expected. The PS sample was prepared via bulk polymerization with an MMT treated with a dimethyl, *n*-hexadecyl, 4-vinylbenzyl ammonium salt (VB16–MMT).[25] Indeed, the PS sample was not as uniform in microscale dispersion as the PA-6 sample, perhaps because the amount of clay loading in this sample was lower (mass fraction = 3%). Because no shear was applied to this

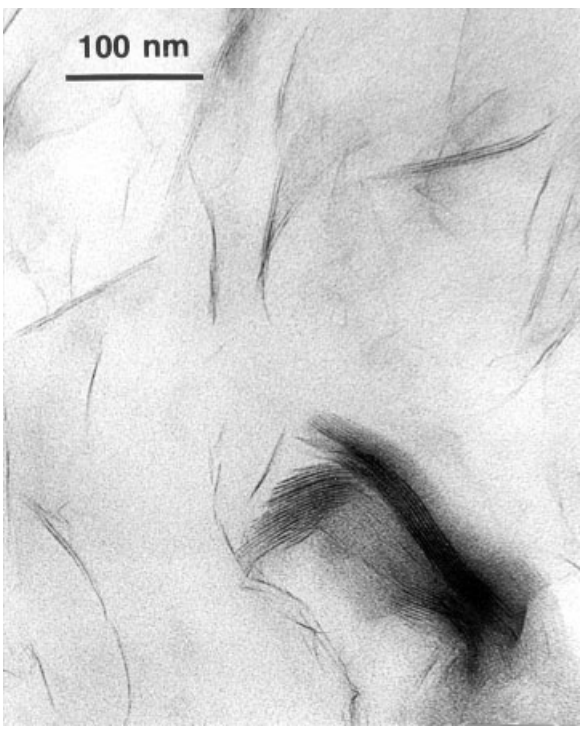

Figure 10 High-magnification TEM image of a PPgMA intercalated/exfoliated nanocomposite (mass fraction = 8% A–MMT).

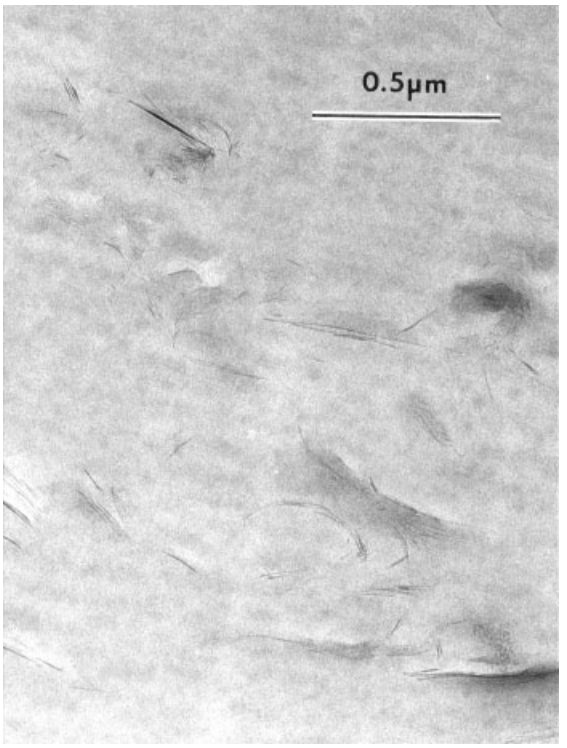

Figure 11 Low-magnification TEM image of an exfoliated PS nanocomposite (mass fraction = 3% VB16–MMT).

Figure 13 High-magnification TEM image of an exfoliated PS nanocomposite (mass fraction = 3% VB16–MMT).

sample, the exfoliated regions were not uniformly dispersed throughout the sample. The largest difference between these two samples was the overall order of the exfoliated layers. In the PS sample (Fig. 13), one could see the long-range order of the original clay tactoid. During polymerization to make this nanocomposite, the polymer entered the gallery to push the clay layers apart such that the *d*-spacing could not be observed by XRD. This phenomena has also been seen with exfoliated epoxy samples.[36] Because there was no shear involved in the preparation of this sample, the original order of the clay tactoid remained, even though the *d*-spacing could not be observed by XRD. Because this order could not be observed at wide angles with XRD, small-angle XRD may show the order, as it has for other materials.[37] The PA-6 sample was prepared with an *in situ* polymerization approach with an MMT treated with a 12-amino-1-dodecanoic acid ammonium salt (AcidC12–MMT). Specifically, the clay was dispersed in the monomer before polymerization, and the polymerization process expanded the clay layers. However, this sample was subjected to shear after the polymerization process via processing in a twin-screw extruder to pelletize it after synthesis in a polymer reactor. This shear disordered the clay layers, giving the structure observed in Figure 14. The difference between an ordered and disordered exfoliated PLSN is a minor one, as both have single clay layers in the polymer matrix. As seen with the PA-6 sample, exfoliated materials that start with order between MMT layers can lose that order with melt processing under shear.

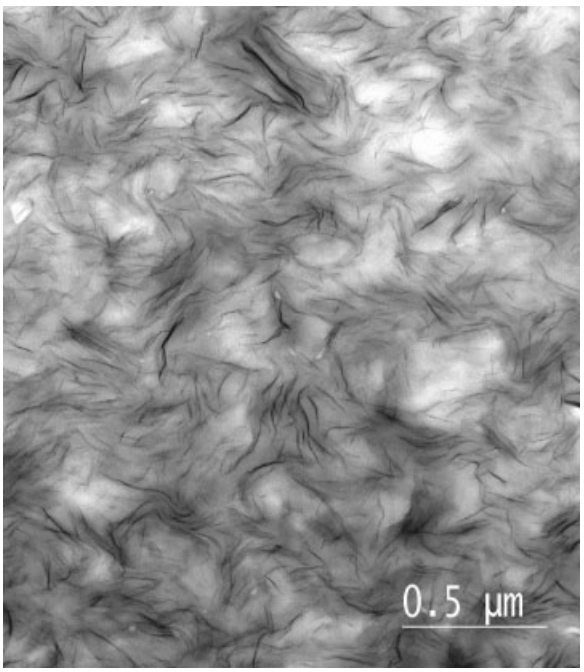

Figure 12 Low-magnification TEM image of an exfoliated PA-6 nanocomposite (mass fraction = 5% AcidC12–MMT).

Figure 14 High-magnification TEM image of an exfoliated PA-6 nanocomposite (mass fraction = 5% AcidC12–MMT).

CONCLUSIONS

We have shown several different PLSNs of varying nanoscale dispersions, comparing and contrasting the results by XRD and TEM. In light of these results, the definitions used to describe PLSNs should be modified to more accurately describe the dispersion at the nanoscale. Two of the definitions are still quite useful in describing the nature of the PLSN, namely, immiscible and exfoliated. To avoid confusion, immiscible systems should probably be described as microcomposites rather than as immiscible nanocomposites. The exfoliated systems do fall into two categories, exfoliated ordered (PS) and exfoliated disordered (PA-6). The greatest clarification is needed for the intercalated definition. Although some purely intercalated nanocomposites have been made,[38] they are not very common. As exfoliated nanocomposites are generally the desired product of PLSN synthesis, attempts that do not achieve exfoliation often fall into this mixed morphology category. The most important observation determined from this study is that XRD results by themselves cannot be used to adequately describe the nanoscale dispersion of the layered silicate present in PLSNs. XRD results when properly interpreted and combined with TEM results give a much clearer picture of the actual nanoscale dispersion and overall global dispersion of the clay in the polymer. Further, these two techniques provide information to help derive meaningful relationships between the PLSN nanostructure and macroscale properties.

The authors thank Terrell Vanderah of the National Institute of Standards and Technology–Materials Science & Engineering Laboratory for use of the Ceramics Division XRD facilities. TEM analysis on the PA-6 nanocomposites was performed by Joseph Harris of The Dow Chemical Company; his assistance and that of his company is gratefully acknowledged. Finally, the authors thank Southern Clay Products for the donation of several MMT clays and for technical assistance.

References

1. Giannelis, E. P. Adv Mater 1996, 8, 29.
2. Wang, Z.; Pinnavaia, T. J Chem Mater 1998, 10, 1820.
3. Burnside, S. D.; Giannelis, E. P. Chem Mater 1995, 7, 1597.
4. Alexandre, M.; Dubois, P. Mater Sci Eng 2000, 28, 1.
5. Gilman, J. W. Appl Clay Sci 1999, 15, 31.
6. Gilman, J. W.; Kashiwagi, T.; Nyden, M.; Brown, J. E. T.; Jackson, C. L.; Lomakin, S.; Giannelis, E. P.; Manias, E. Chemistry and Technology of Polymer Additives; Royal Society of Chemistry: Cambridge, England, 1999; p 249.
7. Gilman, J. W.; Jackson, C. L.; Morgan, A. B.; Harris, R., Jr.; Manias, E.; Giannelis, E. P.; Wuthenow, M.; Hilton, D.; Phillips, S. H. Chem Mater 2000, 12, 1866.
8. Gunter, M.; Reichert, P.; Mülhaupt, R.; Gronski, W. Polym Mater Sci Eng 2000, 82, 228.
9. Davis, R. D.; Jarrett, W. L.; Mathias, L. J. Polym Mater Sci Eng 2000, 82, 272.
10. VanderHart, D. L.; Asano, A.; Gilman, J. W. Chem Mater 2001, 13, 3781.
11. VanderHart, D. L.; Asano, A.; Gilman, J. W. Chem Mater 2001, 13, 3796.
12. Krishnamoorti, R.; Vaia, R. A.; Giannelis, E. P. Chem Mater 1996, 8, 1728.
13. Giannelis, E. P.; Burnside, S. D. J Polym Sci Part B: Polym Phys 2000, 38, 1594.
14. Huang, X.; Lewis, S.; Brittain, W. J.; Vaia, R. A. Macromolecules 2000, 33, 2000.
15. Reichert, P.; Nitz, H.; Klinke, S.; Brandsch, R.; Thomann, R.; Mülhaupt, R. Macromol Mater Eng 2000, 275, 8.
16. Vaia, R. A.; Jandt, K. A.; Krammer, E. J.; Giannelis, E. P. Chem Mater 1996, 8, 2628.
17. Müller, U. Inorganic Structural Chemistry; Wiley: New York, 1992; p 173.
18. Ginzburg, V. V.; Singh, C.; Balazs, A. C. Macromolecules 2000, 33, 1089.
19. Xie, W.; Gao, Z.; Pan, W.-P.; Hunter, D.; Singh, A.; Vaia, R. Chem Mater 2001, 13, 2979.
20. Pauly, T. R.; Pinnavaia, T. J Chem Mater 2001, 13, 987.
21. Kruk, M.; Jaroniec, M.; Sayari, A. J Phys Chem B 1999, 103, 4590.
22. Dennis, H. R.; Hunter, D. L.; Chang, D.; Kim, S.; White, J. L.; Cho, J. W.; Paul, D. R. Soc Plast Eng Annu Tech Conf 2000, 1, 428.
23. Chen, G.; Qi, Z.; Shen, D. J Mater Res 2000, 15, 351.
24. Okamoto, M.; Morita, S.; Taguchi, H.; Kim, Y. H.; Kotaka, T.; Tateyam, H. Polymer 2000, 41, 3887.
25. Morgan, A. B.; Gilman, J. W.; Jackson, C. L. Macromolecules 2001, 34, 2735.
26. Morgan, A. B.; Gilman, J. W.; Jackson, C. L. Polym Mater Sci Eng 2000, 82, 270.
27. Lee, J.; Takekoshi, T.; Giannelis, E. Mater Res Soc Symp Proc 1997, 457, 513.

28. Ishida, H.; Campbell, S.; Blackwell, J Chem Mater 2000, 12, 1260.
29. Vaia, R. A.; Weathers, M. S.; Bassett, W. A. Powder Diffraction 1994, 9, 44.
30. Morgan, A. B.; Gilman, J. W.; Nyden, M.; Jackson, C. L. National Institute of Standards and Technology Internal Report 6465; National Institute of Standards and Technology: Gaithersburg, MD, 2000.
31. Gilman, J. W.; Harris, R. H.; Hunter, D. Presented at the 44th International SAMPE Symposium and Exhibition, Long Beach, CA, May 1999.
32. Zhu, J.; Morgan, A. B.; Lamellas, F.; Wilkie, C. A. Chem Mater, 2001, 13, 4649.
33. Kojima, Y.; Usuki, A.; Kawasumi, M.; Okada, A.; Fukushima, Y.; Kurauchi, T.; Kamigaito, O. J Mater Res 1993, 8, 1185.
34. Reynolds, R. C., Jr. Diffraction by Small and Disordered Crystals in Modern Powder Diffraction; Reviews in Mineralogy Vol. 20; Mineralogical Society of America: Washington, DC, 1989; p 144.
35. Klug, H. P.; Alexander, L. E. X-Ray Diffraction Procedures; Wiley: New York, 1974.
36. Brown, J. M.; Curliss, D.; Vaia, R. A. Chem Mater 2000, 12, 3376.
37. Vaia, R. A.; Lincoln, D.; Wang, Z.-G.; Hsiao, B. S. Polym Mater Sci Eng 2000, 82, 257.
38. Gilman, J. W.; Kashiwagi, T.; Morgan, A. B.; Harris, R. H.; Brassel, L. D.; VanLandingham, M.; Jackson, C. L. National Institute of Standards and Technology Internal Report 6531; National Institute of Standards and Technology: Gaithersburg, MD, 2000.